Type-II InGaN-GaNAs quantum wells for lasers applications

Ronald A. Arif,[a] Hongping Zhao, and Nelson Tansu[b]
Center for Optical Technologies, Department of Electrical and Computer Engineering, Lehigh University, 7 Asa Drive, Bethlehem, Pennsylvania 18015, USA

(Received 12 November 2007; accepted 6 December 2007; published online 2 January 2008)

We present a visible III-nitride gain medium based on type-II InGaN-GaNAs quantum well (QW), employing thin dilute-As (~3%) GaNAs layer. The utilization of GaNAs layer shifts the hole confinement to the center of the type-II QW, which significantly reduces the charge separation effect. The optical gain and spontaneous recombination rate of the type-II InGaN-GaNAs QW are analyzed and compared with those of conventional InGaN QW emitting in the blue regime ($\lambda \sim 450$ nm), using six-band $\boldsymbol{k.p}$ formalism for energy dispersion of the III-nitride wurtzite semiconductor. The use of type-II QW leads to significant improvement in the optical gain and spontaneous recombination rate. © *2008 American Institute of Physics*. [DOI: 10.1063/1.2829600]

III-nitride active media for visible lasers and light emitting diodes (LEDs) are mainly based on type-I InGaN quantum wells (QWs).[1,2] One of the major challenges for the conventional InGaN/GaN QW is the large spontaneous and piezoelectric polarization fields in QW. These lead to charge separation, which significantly reduce the optical gain of the QW. To minimize electrostatic field, nonpolar InGaN material growths have been pursued.[3] Approaches to minimize the charge separation effect via δ-AlGaN layer in InGaN QW[4] and staggered InGaN QW[5,6] with improved electron-hole wavefunction overlap (Γ_{e_hh}), have resulted in improvement in the efficiency and output power of LEDs. In this paper, we present a visible gain medium based on type-II InGaN-GaNAs QW with significantly enhanced transition matrix element, which will lead to large improvement in its optical gain and radiative recombination rate.

Based on Fermi's Golden Rule, the radiative recombination rate of the interband transition is proportional to the square of the Γ_{e_hh}. In conventional type-I InGaN QW, the spontaneous and piezoelectric polarization fields result in energy band-bending, which leads to charge separation in QW. By engineering the energy band lineup and polarization field using nitride-based type-II QW with improved overlap (Γ_{e_hh}), its radiative recombination rate and optical gain of III-nitride QWs can be enhanced.

The GaSb-based type-II "W" QW[7,8] and dilute-nitride type-II InGaN-GaNAs QW[9,10] active regions have been employed for laser applications in midinfrared and 1550 nm regimes, respectively. Our proposed type-II InGaN-GaNAs QW structure is formed by sandwiching a thin dilute-As (As<5%) GaNAs layer with InGaN QW layers. Single-phase, hexagonal GaNAs specular thin film with up to 6.7% As content have been recently synthesized by metalorganic chemical vapor deposition (MOCVD).[11] The studies on dilute-As incorporation into GaN show hybridization of the localized As states and the GaN valence band leads to a formation of a new valence band with transitional gap of 2.5–2.7 eV.[12] This bandgap reduction and band lineup of N-rich GaNAs layer can then be exploited—utilizing type-II InGaN-GaNAs QW—to mitigate the impact of the polarization field to maintain a large Γ_{e_hh}. For instance, the addition of 2% As into GaN layer leads to the resulting transitional energy gap of the GaNAs alloy reduced down to ~2.7 eV, which is 700 meV lower than that of bulk GaN.[12]

Figures 1(a) and 1(b) show the comparison of the energy band lineups at the zone center ($k_t=0$) of the conventional

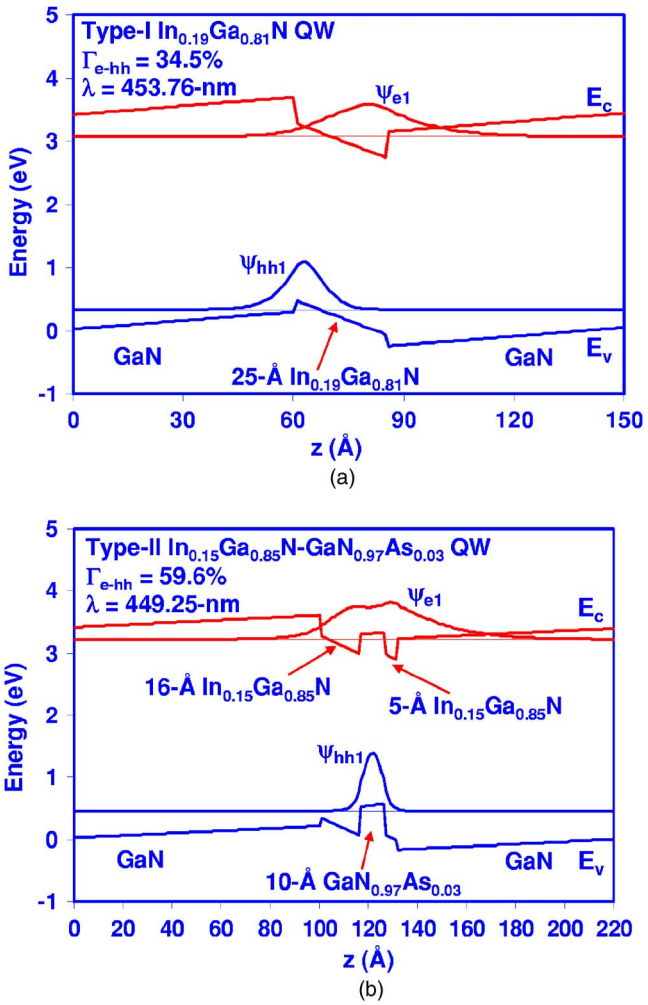

FIG. 1. (Color online) Energy band lineup of (a) type-I $In_{0.19}Ga_{0.81}N$ QW and (b) type-II $In_{0.15}Ga_{0.85}N-GaN_{0.97}As_{0.03}$ QW. Both structures are designed for $\lambda \sim 450$ nm. Note the 1.72× improvement in the wavefunction overlap Γ_{e_hh} in the type-II QW structure.

[a]Electronic mail: raa4@lehigh.edu.
[b]Electronic mail: tansu@lehigh.edu.

 © 2008 American Institute of Physics
Downloaded 20 Jul 2011 to 128.180.137.141. Redistribution subject to AIP license or copyright; see http://apl.aip.org/about/rights_and_permissions

type-I 25 Å $In_{0.19}Ga_{0.81}N$ QW (Γ_{e_hh}=34.5%) with that of the type-II 16 Å $In_{0.15}Ga_{0.85}N$/10 Å $GaN_{0.97}As_{0.03}$/5 Å $In_{0.15}Ga_{0.85}N$ QW (Γ_{e_hh}=59.6%), with both active regions designed to emit at $\lambda \sim 450$ nm. The ground state electron and hole eigenenergies and their respective wavefunctions are also shown in Figs. 1(a) and 1(b). Although both structures are designed for emission in the blue ($\lambda \sim 450$ nm) regime, the use of type-II QW leads to several advantages as follows: (1) less amount of In content in the QW is required than that of the conventional QW structure, and (2) it offers improvement in the Γ_{e_hh} by 1.72 times. By utilizing a thin (10 Å) N-rich GaNAs layer, the hole wave function shifts to the center of the type-II QW structure, thus, greatly reducing the charge separation effect. The deep hole confinement (~460 meV) from the InGaN-GaNAs QW also leads to suppression of carrier leakage.

From the MOCVD growth perspective, the GaNAs film was grown at 700–750 °C,[11] which is compatible with the growth temperature of InGaN QW. The x-ray diffraction measurement comparing the 2θ peaks of [0002] GaN and [0002] GaNAs indicates that the strain $\Delta a/a$ in the $GaN_{0.97}As_{0.03}$ grown on GaN is compressive at +0.78%,[11] which is much smaller than that typically found in the InGaN-GaN QW ($\Delta a/a$=+2–2.5%). As the proposed type-II QW structure requires very thin (~10 Å) and minimum As-content (2–3%) GaNAs, the MOCVD growth should be feasible.

For the calculation of the transition matrix element, the energy subband dispersion is obtained by using 6×6 $\boldsymbol{k.p}$ formalism for wurtzite semiconductor[13] taking into account valence band mixing (heavy hole, light hole, and crystal field split off hole), strain effects, and spontaneous and piezoelectric polarization fields. The spontaneous recombination rate and optical gain can then be calculated following the treatment presented in Ref. 14, using the linewidth broadening of 0.1 ps up to transverse wavevector $k_t \sim 0.2$ Å^{-1}. The band parameters for the III-nitride alloys were obtained from Refs. 13–19. The GaN electron effective mass constants of $0.18m_o$ and $0.2m_o$ were used for the *c*-axis and transverse direction, respectively.[16] The InN electron effective mass of $0.11m_o$ was used for both the *c* axis and transverse directions.[16] The energy gap of the InGaN QW is calculated using bowing parameter of 1.4 eV (Ref. 17) and InN energy gap of 0.6405 eV,[17] with ΔE_c:ΔE_v of 70:30.[18,19] In developing the valence band hybridization model of N-rich GaNAs alloy, a flat conduction band alignment was assumed between GaN and GaNAs.[12] The energy gap of the dilute-As $GaN_{1-y}As_y$ alloy can be linearly extrapolated from experiments for low As-content (y) up to 6.7%,[12] as follows (in eV):

$$E_{g\_GaNAs}(y) = -4.565 \times y + 2.7978 \quad (\text{for } 0 < y < 0.067). \tag{1}$$

The spontaneous emission spectra and optical gain of the conventional type-I InGaN QW and the type-II InGaN-GaNAs QW structures have been calculated and compared for increasing carrier density, $n=1-5\times10^{19}$ cm^{-3}, as shown in Figs. 2(a) and 2(b), respectively. Both gain and spontaneous recombination rate are obtained by including all possible transitions between electron and hole confined states. Note that the polarization field-induced band bending in the III-nitride QW leads to the breaking of the orthogonality condition between states with different quantum number and, therefore, these terms have to be included in the gain and spontaneous emission calculation. From our calculation, we observed that the improvements in the peak spontaneous emission spectra and peak optical gain by ~3 times were found for the type-II InGaN-GaNAs QW.

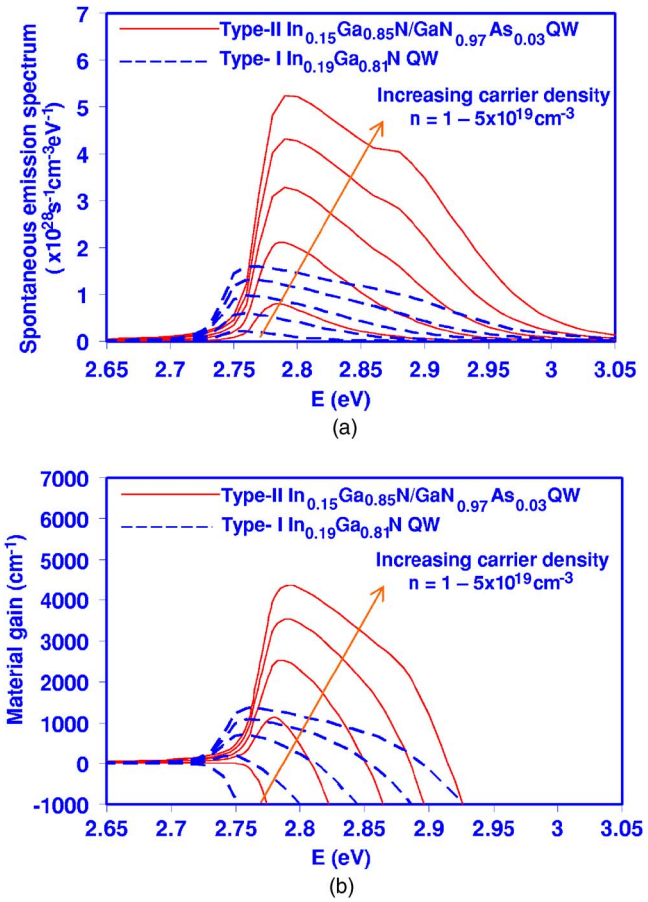

FIG. 2. (Color online) (a) Spontaneous emission spectra and (b) optical gain type-I $In_{0.19}Ga_{0.81}N$ QW and type-II $In_{0.15}Ga_{0.85}N-GaN_{0.97}As_{0.03}$ QW emitting at ~450 nm for increasing carrier density $n=1-5\times10^{19}$ cm^{-3}.

The peak material gains (g_p) as a function of carrier density are shown in Fig. 3 for both the conventional and staggered structures at room temperature. The transparency carrier densities (n_{tr}) for the type-II QW structure is found as 1.41×10^{19} cm^{-3}, which is slightly reduced in comparison to that ($n_{tr}=1.614\times10^{19}$ cm^{-3}) of conventional QW. The differ-

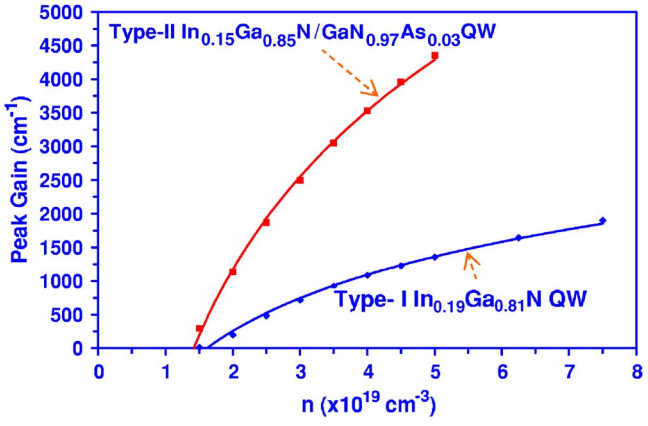

FIG. 3. (Color online) Peak material gain (g_p) as a function of carrier density for type-I $In_{0.19}Ga_{0.81}N$ QW and type-II $In_{0.15}Ga_{0.85}N-GaN_{0.97}As_{0.03}$ QW at room temperature.

Downloaded 20 Jul 2011 to 128.180.137.141. Redistribution subject to AIP license or copyright; see http://apl.aip.org/about/rights_and_permissions

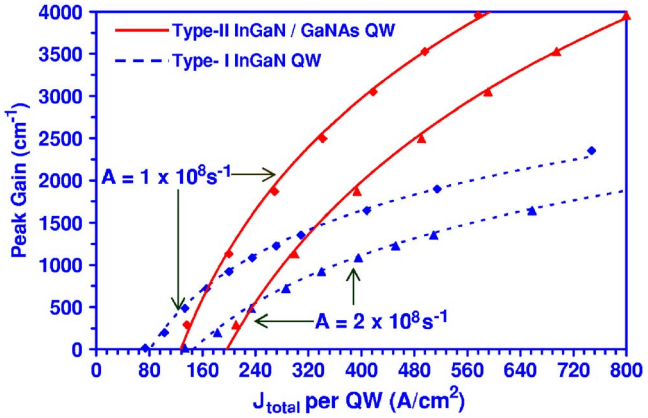

FIG. 4. (Color online) Peak material gain (g_p) as a function of current density (J_{total}) per QW for type-I $In_{0.19}Ga_{0.81}N$ QW and type-II $In_{0.15}Ga_{0.85}N-GaN_{0.97}As_{0.03}$ QW at room temperature.

ential gains (dg/dn) near transparency for the type-II QW and conventional type-I QW are found as 2.4×10^{-16} and 7.47×10^{-17} cm^2, respectively. From our studies, the peak optical gain of the type-II QW structures ($g=4290$ cm^{-1}, for $n=5\times10^{19}$ cm^{-3}) exhibit significant improvement, in comparison to that of conventional InGaN QW ($g=1363$ cm^{-1}, for $n=5\times10^{19}$ cm^{-3}). The improvement in the material gain and differential gain in the type-II QW structure can be attributed to its larger Γ_{e_hh} and momentum matrix element.

To analyze the feasibility of the type-II QW active region for laser implementation, we employ a four-stage QW active region in typical III-Nitride laser structure with optical mode confinement factor (Γ_{opt}) and internal loss (α_i) of 0.04 and 27 cm^{-1}, respectively. For uncoated laser structures with 500 μm cavity length (corresponding to mirror loss $\alpha_m\sim33.06$ cm^{-1}), the threshold gain (g_{th}) per QW of ~1500 cm^{-1} is required for lasing action. Referring to the gain relation in Fig. 3 for type-II QW, the calculated threshold carrier density (n_{th}) is $\sim2.2\times10^{19}$ cm^{-3}, which corresponds to $\sim60\%$ reduction in comparison to that ($n_{th}\sim5.62\times10^{19}$ cm^{-3}) for conventional InGaN QW.

The radiative recombination current density (J_{Rad}) for the QW can be obtained by integrating the spontaneous emission spectra in Fig. 2(a). The total recombination mechanisms include both the radiative and nonradiative recombination processes. In our analysis, we only consider the monomolecular current density ($J_{nr}=An$) as the nonradiative term, where A is the monomolecular recombination constant. The Auger current component is neglected, as this recombination is negligible for wide bandgap InGaN QW.[20] As shown in Fig. 4, the calculated optical gain as a function of current density ($J_{Rad}+J_{nr}$) for both the type-II QW and the conventional type-I InGaN QW structures are shown for two different monomolecular recombination constants[21,22] $A=1\times10^8$ s^{-1} and $A=2\times10^8$ s^{-1}. For laser structure with threshold gain (g_{th}) per QW of 1500 cm^{-1}, the use of type-II InGaN-GaNAs QW leads to threshold current density J_{th} (for four QWs) of 905 and 1345 A/cm^2 for the case of $A=1\times10^8$ s^{-1} and $A=2\times10^8$ s^{-1}, respectively, which correspond to reductions of 35% ($J_{th}=1392$ A/cm^2, for $A=1\times10^8$ s^{-1}) and 41% ($J_{th}=2270$ A/cm^2 for $A=2\times10^8$ s^{-1}) in threshold current densities of conventional InGaN QW. The significant reduction of the threshold current density for the type-II QW can be attributed to the improved differential gain and the lower threshold carrier density, which assist in suppressing the nonradiative current density. Recently, Shen *et al.*[23] found Auger recombination current density (J_{Auger}) may play important role in thick InGaN/GaN double-heterostructure ($d_{Active}=10-77$ nm) in particular for high carrier density operation. Note that the Auger coefficient in InGaN-GaN QW system still requires further studies, due to the large discrepancies from the reported Auger coefficients (C_{Auger}) ranging from $0.9-1\times10^{-32}$ (Ref. 20) up to $1.4-2\times10^{-30}$ cm^{-6}/s.[23] However, a significant reduction in threshold carrier density achievable in the type-II QW will be crucial for suppressing the J_{Auger}, as the J_{Auger} is proportional to $\sim n_{th}^3$.

In summary, type-II InGaN-GaNAs QW structure has been proposed and analyzed as improved gain media in the visible regime. The utilization of type-II InGaN–GaNAs QW active region leads to improvement in the peak optical gain and spontaneous recombination rate by ~3 times at 450 nm wavelength regime. In addition to significant reduction in the threshold current density by 35–40%, the type-II QW structure should also be beneficial for (1) devices that require high threshold gain for lasing operation such as microcavity lasers and (2) high-efficiency light emitting diodes for solid state lighting.

The works are supported by Department of Defense-ARL, National Science Foundation (No. 0701421), and P. C. Rossin Professorship Funds.

[1] S. Nakamura, M. Senoh, N. Iwasa, S. Nagahama, T. Yamada, and T. Mukai, Jpn. J. Appl. Phys., Part 2 **34**, L1332 (1995).
[2] W. Zhao, Y. Li, T. Detchprohm, and C. Wetzel, Phys. Status Solidi C **4**, 9 (2007).
[3] R. M. Farrell, D. F. Feezell, M. C. Schmidt, D. A. Haeger, K. M. Kelchner, K. Iso, H. Yamada, M. Saito, K. Fujito, D. A. Cohen, J. S. Speck, S. P. DenBaars, and S. Nakamura, Jpn. J. Appl. Phys., Part 2 **46**, L761 (2007).
[4] J. Park and Y. Kawakami, Appl. Phys. Lett. **88**, 202107 (2006).
[5] R. A. Arif, Y. K. Ee, and N. Tansu, Appl. Phys. Lett. **91**, 091110 (2007).
[6] R. A. Arif, Y. K. Ee, and N. Tansu, "Nanostructure engineering of staggered InGaN quantum wells light emitting diodes emitting at 420–510 nm," Phys. Status Solidi A (to be published).
[7] J. R. Meyer, C. A. Hoffman, F. J. Bartoli, and L. R. Ram-Mohan, Appl. Phys. Lett. **67**, 757 (1995).
[8] I. Vurgaftman, C. L. Felix, W. W. Bewley, D. W. Stokes, R. E. Bartolo, and J. R. Meyer, Philos. Trans. R. Soc. London, Ser. A **359**, 489 (2001).
[9] N. Tansu and L. J. Mawst, IEEE J. Quantum Electron. **39**, 1205 (2003).
[10] I. Vurgaftman, J. R. Meyer, N. Tansu, and L. J. Mawst, Appl. Phys. Lett. **83**, 2742 (2003).
[11] A. Kimura, C. A. Paulson, H. F. Tang, and T. F. Kuech, Appl. Phys. Lett. **84**, 1489 (2004).
[12] J. Wu, W. Walukiewicz, K. M. Yu, J. D. Denlinger, W. Shan, J. W. Ager III, A. Kimura, H. F. Tang, and T. F. Kuech, Phys. Rev. B **70**, 115214 (2004).
[13] S. L. Chuang and C. S. Chang, Phys. Rev. B **54**, 2491 (1996).
[14] S. L. Chuang, IEEE J. Quantum Electron. **32**, 1791 (1996).
[15] I. Vurgaftman and J. R. Meyer, J. Appl. Phys. **94**, 3675 (2003).
[16] J. Piprek, *Semiconductor Optoelectronic Devices: Introduction to Physics and Simulation* (Academic, London, 2003), p. 34.
[17] J. Wu, W. Walukiewicz, W. Shan, K. M. Yu, J. W. Ager III, S. X. Li, E. E. Haller, H. Lu, and W. J. Schaff, J. Appl. Phys. **94**, 4457 (2003).
[18] J. Piprek and S. Nakamura, IEE Proc.-J: Optoelectron. **149**, 145 (2002).
[19] Y. C. Yeo, T. C. Chong, M. F. Li, and W. J. Fan, J. Appl. Phys. **84**, 1813 (1998).
[20] J. Hader, J. V. Moloney, A. Thranhardt, and S. W. Koch, *Nitride Semiconductor Devices*, edited by J. Piprek (Wiley-VCH, Weinheim, Germany, 2007), Chap. 7, p. 164.
[21] W. W. Chow and M. Kneissl, J. Appl. Phys. **98**, 114502 (2005).
[22] P. Mackowiak and W. Nakwaski, MRS Internet J. Nitride Semicond. Res. **3**, 35 (1998).
[23] Y. C. Shen, G. O. Mueller, S. Watanabe, N. F. Gardner, A. Munkholm, and M. R. Krames, Appl. Phys. Lett. **91**, 141101 (2007).

Downloaded 20 Jul 2011 to 128.180.137.141. Redistribution subject to AIP license or copyright; see http://apl.aip.org/about/rights_and_permissions